Physics of the Earth and Planetary Interiors, 18 (1979) 176–196

ON THE OBSERVABILITY OF ISOTROPIC SEISMIC SOURCES: THE JULY 31, 1970 COLOMBIAN EARTHQUAKE

EMILE A. OKAL [1] and ROBERT J. GELLER [2]

Seismological Laboratory, California Institute of Technology, Pasadena, CA 91125 (U.S.A.)

(Received November 21, 1977; revised and accepted May 17, 1978)

Okal, E.A. and Geller, R.J., 1979. On the observability of isotropic seismic sources: the July 31, 1970 Colombian earthquake. Phys. Earth Planet. Inter., 18: 176–196.

Theoretical calculations are made to study the observability of isotropic components of seismic sources. In particular we consider the 1970 deep Colombian earthquake, for which a precursory isotropic component was previously reported by Gilbert and Dziewonski.

We compare an ultra-long period vertical record at Pasadena of the 1970 event to synthetic seismograms calculated both for Gilbert and Dziewonski's source model and for the pure double-couple source of Furumoto and Fukao, and obtain better overall agreement for the latter. The amplitude of the long-period synthetic for the isotropic source is about 5–15 times smaller than the synthetic for the deviatoric source, suggesting that the data may be relatively insensitive to the presence of a small isotropic source. When this possibility was tested, the overall agreement was found to be almost completely insensitive to the presence of even a reasonably large isotropic component.

However, the isotropic source was derived from multi-station moment tensor inversion, rather than from single-station studies. A numerical experiment on the effect of lateral heterogeneity of eigenfrequencies and of Q on the inversion for the moment tensor shows that even relatively small amounts of heterogeneity can produce spurious isotropic sources from moment tensor inversion.

1. Introduction

The purpose of this paper is to study the observability of isotropic components of the source mechanism of earthquakes having much larger deviatoric moments. As a particular example, we will study the 1970 deep Colombian earthquake, which was the largest deep shock in the past twenty years. The mechanism of this earthquake has been the subject of considerable discussion since Dziewonski and Gilbert (1974) reported that the main earthquake source was preceded by a slow isotropic precursor. There was later extensive discussion of this result (Geller, 1974; Hart and Kanamori, 1975; Kennett and Simons, 1976; Mendiguren, 1977).

Present addresses:
[1] Department of Geology and Geophysics, Yale University, New Haven, CT 06520, U.S.A.
[2] Department of Geophysics, Stanford University, Stanford, CA 94305, U.S.A.

The extensive discussion of the possible isotropic source is a reflection of the important geophysical consequences of this result. From thermodynamic considerations, there must be compressive volume changes in the downgoing lithosphere. It generally has been assumed that the phase changes have too large a time constant to be seismologically observable (Dennis and Walker, 1965; Sykes, 1968). However, some petrological models predict rapid phase changes which might be observable (e.g., Vaišnys and Pilbeam, 1976).

The possibility of isotropic components of earthquake sources has been studied by many investigators. Early efforts by Japanese seismologists are summarized by Matuzawa (1964). Benioff (1964) suggested a volume change of 3% as part of a possible mechanism for a deep Peruvian earthquake. Randall and Knopoff (1970) found both implosive and explosive components in deep earthquakes. The

explosive sources cannot be reconciled with phase changes in the downgoing lithosphere. In this paper, we first present a general discussion of the excitation of seismic waves by isotropic sources, and discuss the Colombian deep earthquake in detail. We then conduct numerical experiments on the effect of various possible systematic biases such as lateral heterogeneity of phase velocity or Q on inversion for the moment tensor. We concentrate on the question of whether lateral heterogeneity could cause isotropic sources as an artifact of moment tensor inversion.

2. The relative efficiency of deviatoric and isotropic sources

The excitation of the earth's normal modes by seismic sources has been extensively studied. Alterman et al. (1959) solved the problem for a simple source. Saito (1967) and Takeuchi and Saito (1972) found expressions for the amplitudes of the earth's spheroidal and torsional normal modes excited by arbitrary combinations of point forces, couples with moment, double-couples and dipoles without moment. Abe (1970) applied Saito's results to the analysis of the free oscillations excited by the 1963 Kurile Islands earthquake. Other derivations of the excitation of normal modes were given by Gilbert (1970) and Gilbert and Dziewonski (1975), and also by Phinney and Burridge (1973).

A complete synthetic seismogram can be calculated by summing all the normal modes of the earth (both the fundamental branches and all the overtones) where the amplitude of each mode is determined from the source type and depth. Y. Satô and his colleagues were the first to calculate synthetics in this way; their results are summarized by Landisman et al. (1970). In order to study the conditions under which isotropic sources can be observed, we will first study the relative amplitudes of the fundamental-mode Rayleigh waves and overtones excited by shear dislocations and isotropic sources at various depths.

2.1. Rayleigh waves

It is well known that isotropic sources, especially at depth, are less efficient than deviatoric ones in exciting Rayleigh waves, and we will examine this phenomenon quantitatively. In the notation of Kanamori and Cipar (1974), the amplitude of the vertical component of the spheroidal mode ${}_nS_l$ (overtone number n and angular order l), excited by a double-couple is:

$$u_r(\vec{r}, t) = y_1^S(r) \cos_n\omega_l t \; \{K_0 s_R P_l^0 - K_1 q_R P_l^1 + K_2 p_R P_l^2\} \quad (1)$$

where the excitation coefficients K_0, K_1, K_2, depend only on the eigenfunctions at the depth of the source and on the kinetic energy of the mode; the source radiation pattern coefficients, p_R, q_R, s_R depend only on the geometry of the source and the azimuth ϕ of the station; and P_l^m is the associated Legendre function of azimuthal order m and angular order l. λ is the fault slip angle, and δ the fault dip as defined by Kanamori and Cipar and y_1^S is the vertical displacement eigenfunction. K_1 is the excitation coefficient for a vertical dip-slip fault ($\lambda = 90°; \delta = 90°; s_R = p_R = 0, q_R = -\sin\phi$) and K_2 for a vertical strike-slip fault ($\lambda = 0°, \delta = 90°; s_R = q_R = 0, p_R = \sin\phi$). The coefficient $s_R = \frac{1}{2}\sin\lambda \sin 2\delta$ is non-zero for any non-vertical fault plane having a dip-slip component. Expressions for K_0, K_1 and K_2 are given by Kanamori and Cipar (1974).

For an isotropic source (taken as positive in the case of an explosion), the vertical displacement is obtained from Takeuchi and Saito (1972):

$$u_r(\vec{r}, t) = y_1^S(r) \cos_n\omega_l t \; N_0 \cdot P_l^0 \quad (2)$$

N_0 is proportional to the radial factor of dilatation (Harkrider, 1964; Gilbert, 1970) and is given in explicit form by Okal (1978).

Away from the epicenter and its antipode, and for large values of l, the Legendre functions P_l^0, P_l^1, P_l^2 in eq. 1 can be replaced by their asymptotic expansion:

$$P_l^m(\theta) = (-1)^m l^{m-1/2} [2/(\pi \sin\theta)]^{1/2} \times \cos[(l + 1/2)\theta + m\pi/2 - \pi/4] \quad (3)$$

By using eq. 3 in eq. 1, the approximate relative excitation of a given mode by various types of seismic sources can be studied through the four sets of numbers: $K_0/l^{1/2}$, $N_0/l^{1/2}$, $K_1 l^{1/2}$ and $K_2 l^{3/2}$. Fig. 1 shows the variation of these parameters for the fundamental

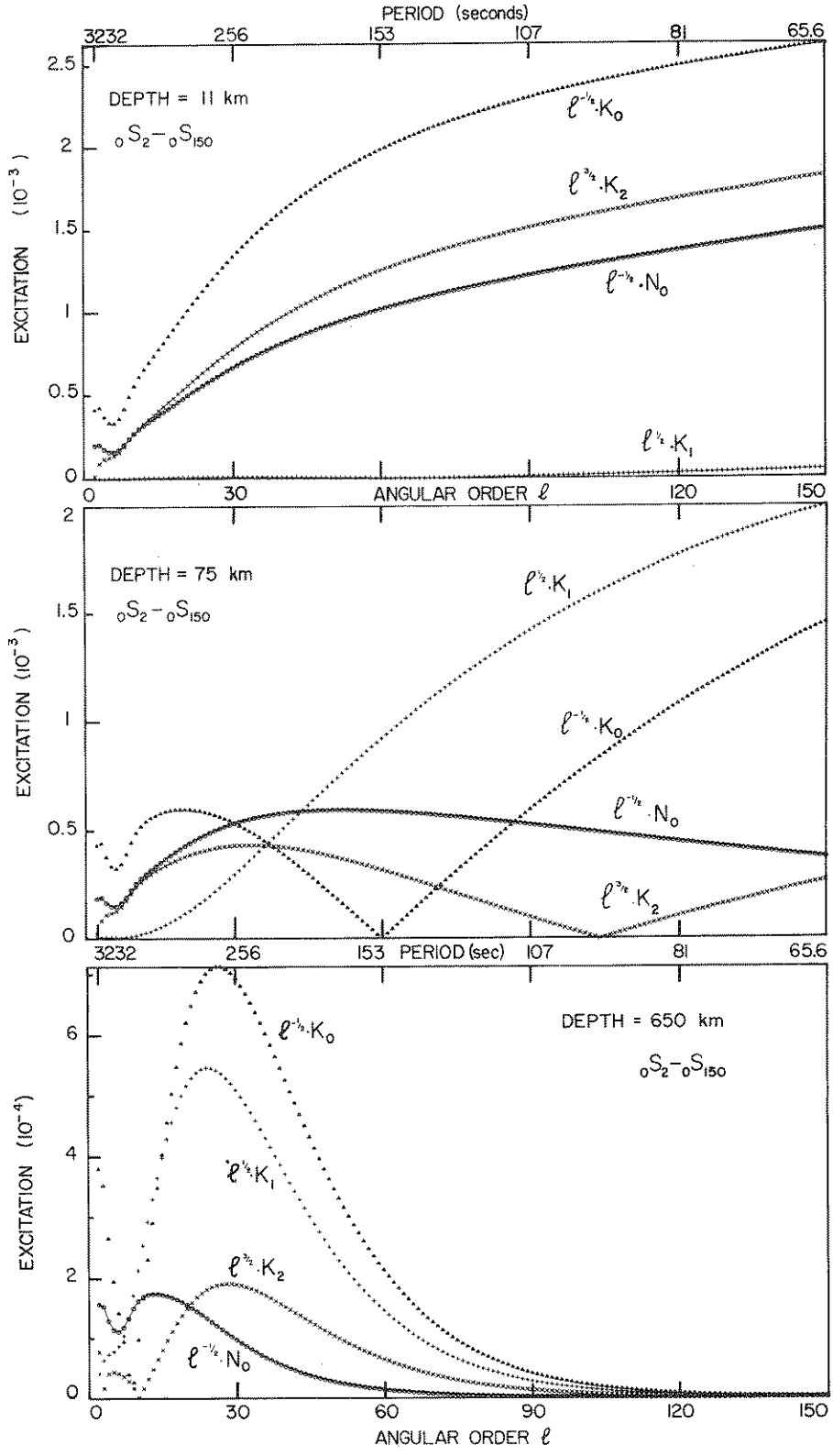

Fig. 1. Values of the excitation coefficients for fundamental spheroidal modes. The excitation coefficients $l^{-1/2}N_0$, $l^{-1/2}K_0$, $l^{1/2}K_1$, $l^{3/2}K_2$ are directly related to the average amplitude of Rayleigh waves at the earth's surface.

spheroidal modes (Rayleigh waves) for three different source depths: 11, 75 and 650 km. The excitation coefficients N_0, K_0, K_1 and K_2 are computed using Gilbert and Dziewonski's (1975) model 1066A, and a moment of 10^{27} dyn cm. For the shallow source, the ratios of $N_0/l^{1/2}$ to $K_0/l^{1/2}$, $K_1 l^{1/2}$ and $K_2 l^{3/2}$ decrease slightly with increasing frequency, but are basically constant. The situation is quite different for the intermediate and deep sources. At a depth of 75 km we find that $N_0/l^{1/2}$ decreases for periods shorter than about 200 s, while the other coefficients are still increasing in value.

The relative excitation for the isotropic source is even weaker for a deep (h = 650 km) source. For all modes with $l > 15$ the coefficient for the isotropic source is much smaller than any of the coefficients for the deviatoric sources, and the isotropic coefficient dies off to a negligible value for a much lower angular order number ($l \simeq 70$) than the deviatoric coefficients ($l \simeq 120$).

The physical reason for the decay of the isotropic coefficient can be illustrated by using the simple case of a Rayleigh wave in a homogeneous half-space. The decay of the wave's amplitude with depth involves two characteristic depths h_ϕ and h_ψ, for the compressional potential ϕ and the shear potential ψ, respectively:

$$\left.\begin{aligned} 1/h_\phi &= \omega(1/c^2 - 1/\alpha^2)^{1/2} \\ 1/h_\psi &= \omega(1/c^2 - 1/\beta^2)^{1/2} \end{aligned}\right| \quad (4)$$

For the case of a Poisson solid ($\alpha = \sqrt{3}\beta$), $1/h_\phi$ = 0.8475 ω/c and $1/h_\psi$ = 0.3933 ω/c. The decay of the total dilatation ϵ_{ii} (and therefore of N_0) is proportional only to ϕ. The decay of any other displacement or stress eigenfunctions involves a sum of terms with the depth dependences of both ϕ and ψ, but ϕ decays much more rapidly with depth than ψ. Thus, no combination of displacements and stresses decays faster with depth than ϵ_{ii} (and N_0) and the ratio N_0/K_i will eventually behave as:

$$\exp[(1/h_\psi - 1/h_\phi)\ \omega z/c]$$

At z = 650 km, this is on the order of 10^{-2} for T = 100 s and 10^{-8} for T = 30 s. Although these figures are clearly only approximations for a spherical, vertically heterogeneous, earth, this example provides physical insight into the relative efficiency of isotropic and dislocation sources. [Jeffreys (1928) used a similar argument to show that deep sources will excite much smaller Rayleigh waves than shallow ones, although he did not distinguish between isotropic and deviatoric sources. Jeffreys' argument was later used by Stoneley (1931) to verify the existence of deep-focus earthquakes on the basis of their small Rayleigh wave amplitudes.]

Fig. 2 shows the relative Rayleigh wave excitation in the form of spectral radiation patterns. From Kanamori and Stewart (1976), the spectral amplitude of the vertical component of Rayleigh waves for a shear dislocation of unit moment is:

$$|U_r(\omega)| = \left(\frac{\pi}{2l \sin \Delta}\right)^{1/2} \cdot \frac{a}{U} \cdot y_1^S(a)$$

$$\times |s_R K_0 - l^2 p_R K_2 - ilq_R K_1| \quad (5)$$

where ω is the frequency (in rd s^{-1}), a is the earth's radius, Δ is the epicentral distance, U is the group velocity and all other variables are defined above.

The corresponding expression for an explosion is:

$$|U_r(\omega)| = \left(\frac{\pi}{2l \sin \Delta}\right)^{1/2} \cdot \frac{a}{U} \cdot y_1^S(a) \cdot |N_0| \quad (6)$$

Although this expression is derived from the asymptotic expansion of the Legendre functions, it is quite accurate, even at very long periods, away from the epicentral and antipodal regions. The spectral radiation patterns plotted in Fig. 2 are for Δ = 60° and a moment of 10^{27} dyn cm. For the shallow source, the radiation pattern amplitudes for three of the different mechanisms are roughly comparable at all three periods shown. In contrast, the amplitudes for the vertical dip-slip fault are negligible because the free surface is a node for this mechanism.

By comparing the spectra for the shallow and deep sources, we can study the frequency and depth dependence for Rayleigh wave excitation. For T = 240 s, the amplitude ratio of the shallow/deep sources is about 2; at T = 150 s the ratio is 10; and at T = 70 s the ratio is 500. The amplitudes for the deep strike-slip fault are about 1/2 of those for the other deep shear dislocations at all three periods, while the relative amplitude for the deep isotropic source grows smaller at shorter periods. The isotropic source amplitude is about 5 times smaller at 240 s, 8 times smaller at 150 s and 17 times smaller at 70 s. Thus the abso-

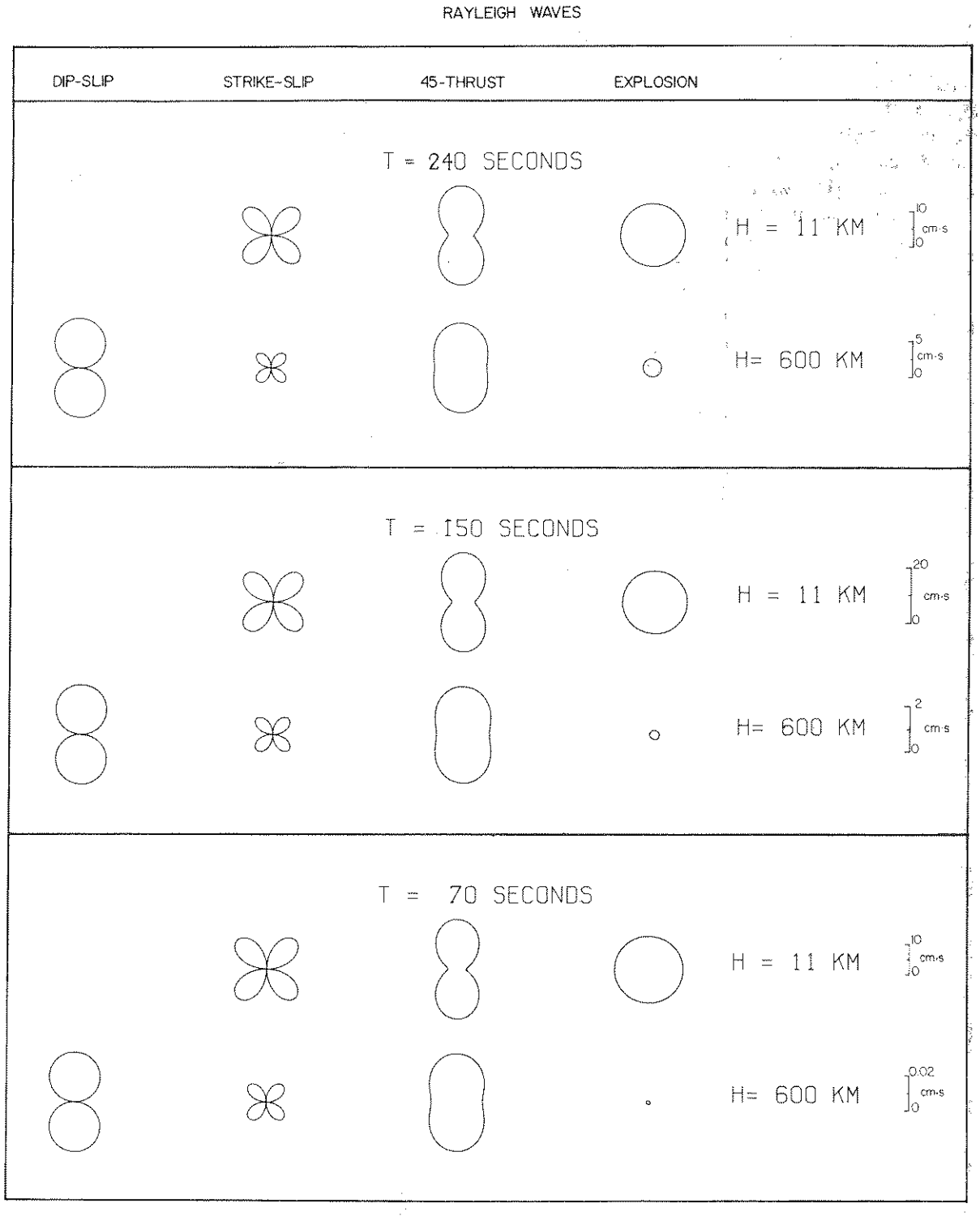

Fig. 2. Spectral radiation patterns of Rayleigh waves for shallow and deep events are compared for various sources. The epicentral distance is $\Delta = 60^\circ$ and a step-function source with a moment of 10^{27} dyn cm is used. The radiation pattern for the shallow dip-slip is not plotted because its amplitude is negligible. The amplitude scales are the same for the four figures on each line, but vary from line to line.

lute amplitude of fundamental mode Rayleigh waves excited by a deep isotropic source decreases extremely rapidly as the period decreases. Even at relatively long periods (70 s), it is extremely difficult to resolve the presence of a deep isotropic source from fundamental mode Rayleigh waves, when a deviatoric source with equal moment is also present.

Isotropic sources are also less efficient than deviatoric sources in exciting the first several higher spheroidal modes. It is possible to characterize the relative efficiency of isotropic sources in exciting each higher mode using the classification scheme of Okal (1978). However, it is much easier to use a body-wave approach to study the excitation of P waves.

2.2. *P waves*

Following Chung and Kanamori (1976) we write the displacement at the earth's surface generated by a point source at depth h and distance Δ as:

$$U(t) = 2\frac{g(\Delta, h)}{a}\frac{R_{\phi,h}}{4\pi\rho_h v_h^3}\dot{M}(t-\tau) \qquad (7)$$

where g is the geometrical spreading factor, a is the earth's radius, ρ_h and v_h are the density and velocity at the hypocenter, $M(t)$ is the moment time function of the source, τ is the travel-time of the P wave to the station, and the factor of 2 is an approximation to the effect of the free surface at the receiver. For an explosion, the radiation pattern coefficient, $R_{\phi,\Delta} = 1$. $R_{\phi,\Delta}$ for dislocation sources is given by Chung and Kanamori.

Fig. 3 compares the P-wave radiation pattern (the Fourier-transform of eq. 7) of an explosion, and three double-couple sources [vertical dip-slip, vertical strike-slip, and 45° dipping thrust ($\delta = 45°$, $\lambda = 90°$)], at both $h = 0$ and $h = 600$ km, at a distance $\Delta = 60°$. A moment of 10^{27} dyn cm, with step-function time dependence, is used. The effect of free-surface reflections above the shallow source (Fukao, 1971; Langston and Helmberger, 1975) is not included.

The scale in Fig. 3 is about a factor of two larger for the top (shallow) sources. In all cases, the excitation of P waves by compressional and deviatoric sources is on the same order of magnitude, reflecting the small dependence of $U(\omega)$ (the Fourier transform of eq. 7) on depth. These results for the excitation efficiency of P waves by the various sources are, to this level of approximation, totally independent of frequency. The spectral amplitudes for Rayleigh waves at periods from 240 to 70 s (from Fig. 2) are about 50–100 times greater than those for the P waves from the shallow source. For the deep source however, the Rayleigh waves are 50 times bigger at $T = 240$ s, but

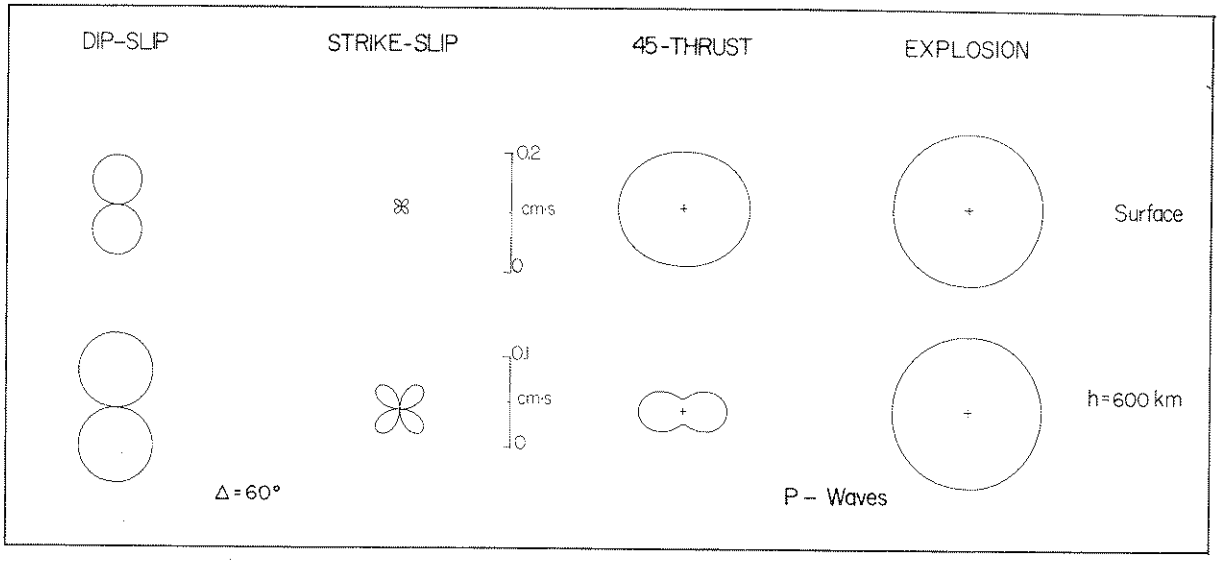

Fig. 3. Spectral radiation pattern of P waves for shallow/deep events are compared for various sources, at a station distance of $\Delta = 60°$. A step-function moment of 10^{27} dyn cm is used for all sources.

the P waves are 5 times bigger at $T = 70$ s.

The relative efficiency of an explosion with respect to a double-couple remains about constant (and on the order of 1) with both depth and frequency for P waves. It decays very rapidly with increasing depth and frequency for Rayleigh waves. The consequences of these differences for the analysis of a deep earthquake are two-fold. First, in order to resolve a possible isotropic component of the seismic moment tensor, an analysis of the body-wave part of the record is desirable. In principle, the possibility of an isotropic source component could also be investigated by studying the high-Q "compressional" overtones (which have a relatively high proportion of compressional energy), and are efficiently excited by isotropic sources (Dratler et al., 1971). However, any interpretation of the amplitudes of the compressional modes may be affected by errors in earth models and lateral heterogeneity, so analysis of the direct P waves is probably preferable.

The relative amplitudes of P waves and surface waves are illustrated in Figs. 4 and 5, which show synthetics starting 7 min after the origin time and lasting 90 min, at a distance of $\Delta = 90^\circ$ for four seismic sources at different depths, computed through summation of spheroidal modes. [Fukao and Abe (1971) presented similar synthetics for fundamental torsional modes.] The geometry of the sources and receiver is summarized in Table I. Fig. 4 uses the ultra-long period "33" instrument in Pasadena (*PAS*): The response of this seismometer is peaked around 160 s. Fig. 5 uses the standard WWSSN "15–100" instrument, whose response is peaked around 20 s. The response curves of these instruments are shown in Fig. 6. The synthetics were obtained by summa-

TABLE I

Geometric parameters of the three double-couple sources used in Figs. 4 and 5

Parameter	Dip-slip	Strike-slip	45-thrust
Dip angle, δ (°)	90	90	45
Slip angle, λ (°)	90	0	90
Azimuth of station with respect to fault (°)	0	45	45
Distance of station (°)	90	90	90
p_R	0	1	0
q_R	−1	0	0
s_R	0	0	0.5

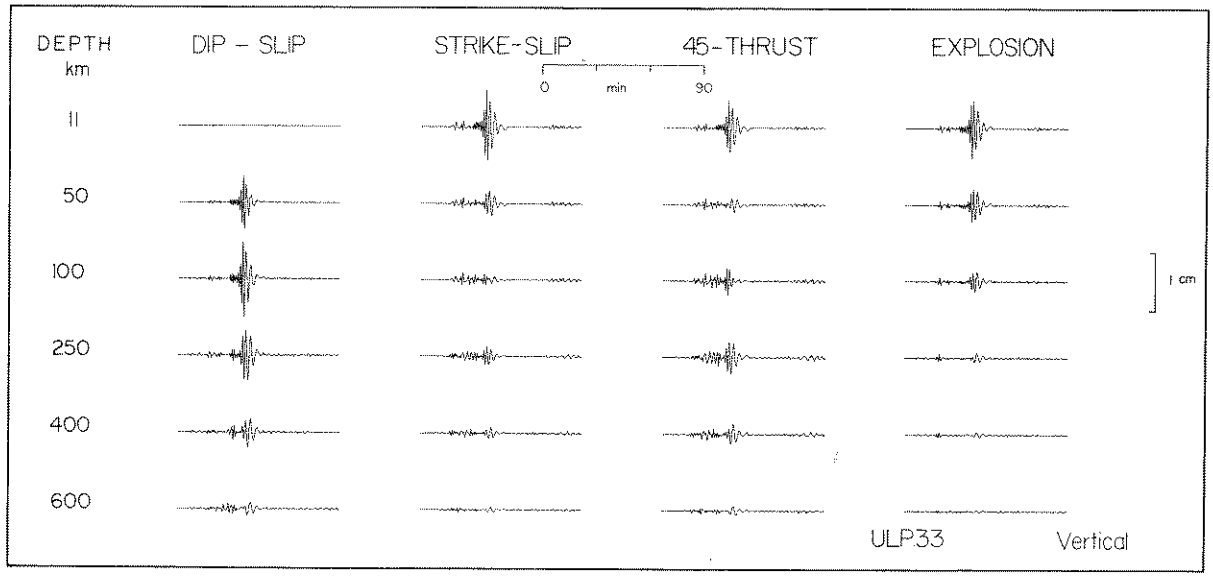

Fig. 4. Vertical-component synthetic seismograms. These seismograms all begin 7 min after the origin time and have a 90-min duration. The epicentral distance is $\Delta = 90^\circ$ and the step-function moment 10^{27} dyn cm, in all cases. The instrument used is the ultra-long period "33" vertical seismometer at *PAS* (see Fig. 6 for its response). The scale is the same for all 24 seismograms.

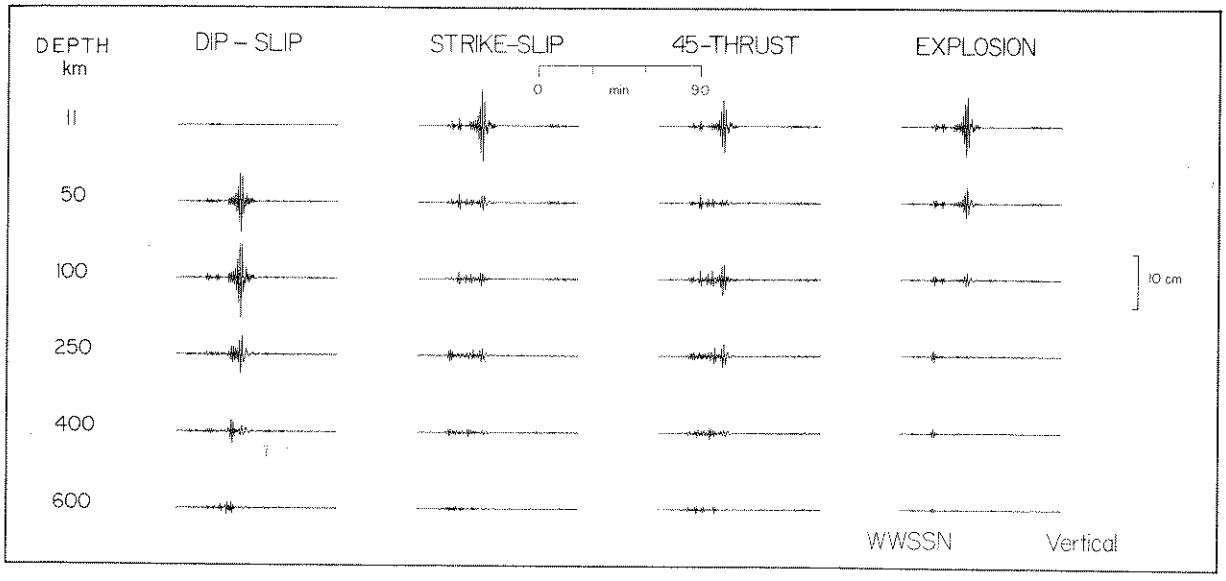

Fig. 5. Same as Fig. 4, but using a WWSSN 15–100 instrument. Note the much faster decay with depth and period of the Rayleigh waves excited by the explosion.

tion of all spheroidal normal modes with frequencies less than 0.0125 Hz; all modes with frequencies greater than 0.0125 Hz ($T < 80$ s) were filtered out, to duplicate the conditions of Gilbert and Dziewonski's (1975) study. (The filter had zero phase shift and decayed linearly from unit amplitude at $T = 120$ s to zero at $T = 80$ s; the same low-pass filter is used for all of the data and synthetics in later sections.) The attenuation of the earth was included by using Anderson and Hart's (1978) model SL2. The same Q model is used in later sections of the present study.

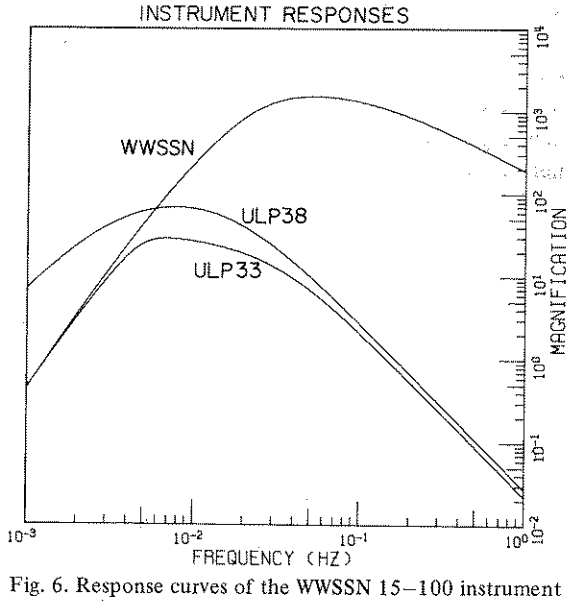

Fig. 6. Response curves of the WWSSN 15–100 instrument and the ultra-long period Pasadena instruments, "ULP33" and "ULP38".

3. Application to the 1970 Colombian earthquake

The Colombian earthquake of July 31, 1970 is the largest deep event to occur in recent times. Its hypocentral parameters, as determined by the USGS are: origin time $17^h08^m05.4^s$ GMT; epicenter 1.5°S, 72.6°W; depth 651 km; $m_b = 7.1$. The latter figure was revised to $m_b = 6.5$ by the ISC. Fig. 7 shows the original record of the event on the vertical ultra-long period "38" seismometer (Gilman, 1960) at *PAS* ($\Delta = 55.1°$, $\phi = 314.1°$). This instrument ($T_0 = 35$ s; $T_g = 270$ s) has peak response at 160 s (see Fig. 6). The usable portion of the record from $17^h00^m00^s$ GMT (about 17 min before the first arrival) to $20^h56^m00^s$ GMT, was digitized at 2-s (later smoothed to 5-s) intervals. The long-period drift of the instrument was removed (see top trace

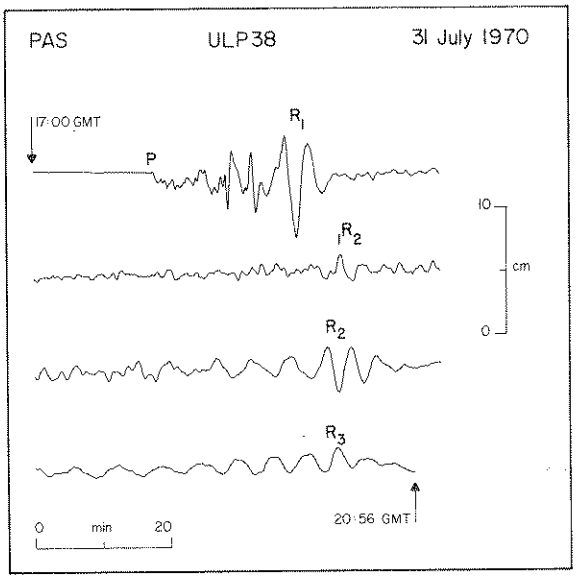

Fig. 7. Original ultra-long period record of the Colombian earthquake at *PAS*. Each line except the bottom is 1 h long.

of Fig. 11) by subtracting the 600-s running average, and the record was then low-pass filtered (see top trace of Fig. 12). Multiple Rayleigh waves (R_1, R_2, R_3) are readily observable, and the $_1R_2$ overtone (the first higher mode, after it has passed the antipode) can be clearly identified (by its group velocity of 5.8 km/s) around 18^h45^m GMT. This record is unique in that it provides both early and later phases which are on-scale and usable.

The focal mechanism of the 1970 Colombian deep shock was initially studied by Mendiguren (1972, 1973) whose first-motion solution requires normal faulting. His solution was later used by Furumoto and Fukao (1976) to investigate the seismic moment of the earthquake (Table II) through the use of synthetic seismograms of fundamental-mode Rayleigh waves. They obtained a value of $M_0 = 2.1 \cdot 10^{28}$ dyn cm, and observed a slight rotation of the surface-wave radiation pattern with respect to the focal mechanism from the body-wave first motions. This rotation had also been reported by Gilbert and Dziewonski (1975) from their inversion results.

The body waves from this event were studied by Furumoto (1977), who found that the primary P waves on WWSSN records were caused by a complex series of multiple events with a duration of about

TABLE II

Moment values for the Colombian earthquake

Study	Moment value (10^{27} dyn cm)
Mendiguren (1972)	11.6
Furumoto and Fukao (1976)	21.0
Furumoto (1977)	24.0
Gilbert and Dziewonski (1975) *	15.3

* Moment value for the D_1 component, on essentially Furumoto and Fukao's fault plane.

60 s, and inferred a total moment of $2.4 \cdot 10^{28}$ dyn cm from the body waves. The excellent agreement of the surface-wave moment (measured at about $T = 200$ s) and the much higher frequency body-wave moment suggests that nearly all of the deviatoric strain release at the source has a duration of only 60 s, and did not include any significant slow slippage of much longer duration. Strelitz (1977) also studied the multiple event mechanism using body waves.

Table III lists the deviatoric focal mechanisms of Mendiguren (1973) and Gilbert and Dziewonski (1975). The source time function used by Furumoto and Fukao (1976) (a ramp of duration 60 s) can be taken as a step function at longer periods. The moment rate functions obtained by Gilbert and Dziewonski are shown in Fig. 10, for the isotropic and both deviatoric sources. They were obtained by resolving the individual principal values of the moment tensor (Gilbert and Dziewonski, 1975; fig. 27, p. 265) into their deviatoric and isotropic components. (The moment rate functions are similar to the "far-field" source functions used in body-wave studies.)

We have neglected the small rotation of the principal axes which occurred during the earthquake and treated the axes as fixed in their average position. The eigenvalues given in fig. 27 of Gilbert and Dziewonski (1975) can be decomposed to give the moment rate of the isotropic source and of two mutually perpendicular double-couples. This decomposition was selected for our plots in Fig. 10, because the double-couple moment rate function D_1 is essentially that for Mendiguren's (1972) and Furumoto and Fukao's (1976) fault geometry, and can be directly compared

TABLE III

Parameters of the deviatoric focal sources used in the synthetics

Source	ϕ (°)	δ (°)	λ (°)	Tensional axis ϕ, δ (°)	Compressional axis ϕ, δ (°)	Moment (10^{27} dyn cm)	Source function
Mendiguren (1973) Furumoto and Fukao (1976)	148	58	−99	244, 103	32, 165	21	step
Gilbert and Dziewonski (1975)							
D_1: 1st deviatoric source	167	68	−87	255, 112	82, 157	see Fig. 8	see Fig. 8
D_2: 2nd deviatoric source	298	76	−19	−14, 93	255, 112	see Fig. 8	see Fig. 8

to their results. D_2 is the moment rate function for the double-couple which accounts for the remainder of the deviatoric source. The P-axis of D_2 is the T-axis of D_1 and the T-axis of D_2 is the intermediate axis of D_1.

The moment of each mechanism is obtained by integrating to find the area under each moment rate curve in Fig. 8. When we performed this integration, we found the moment of D_1 to be $-1.43 \cdot 10^{28}$ dyn cm; of I (the isotropic) to be $-8.2 \cdot 10^{27}$; and of D_2 to be only $-2.8 \cdot 10^{27}$. Our values obtained from the figure in Gilbert and Dziewonski's paper are very different from those they obtained for the deviatoric mechanism. We found the three deviatoric eigenvalues of the moment tensor to be $(-1.43 \cdot 10^{28}, 1.15 \cdot 10^{28}, 0.27 \cdot 10^{28})$ dyn cm, while in their table on p. 266, they list $(-1.53 \cdot 10^{28}, 9.2 \cdot 10^{27}, 6.1 \cdot 10^{27})$ dyn cm. This discrepancy exists because Gilbert and Dziewonski found the final moment values by extrapolating the moment rate spectra to DC, while we found the area under their moment rate curves in the time domain from $t = -200$ s to $t = 200$ s (A.M. Dziewonski, pers. commun., 1977). Outside this range of periods, the moment rate spectrum probably has very poor resolution because of the WWSSN instrument response. Thus, in contrast to Gilbert and Dziewonski, who concluded that the deviatoric mechanism of the Colombian earthquake differed substantially from a double-couple we conclude the intermediate eigenvalue is essentially negligible at long periods, and that the deviatoric mechanism is essentially a double-couple. This conclusion was reached on other grounds by Mendiguren, and Furumoto and Fukao.

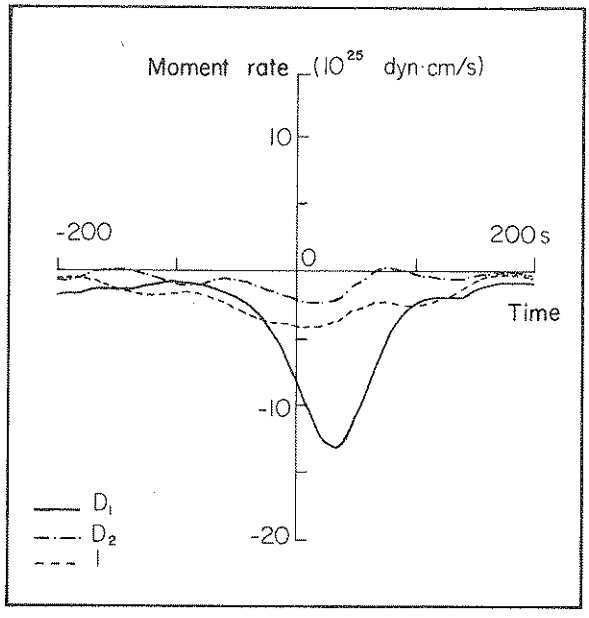

Fig. 8. Moment rate functions of both deviatoric (D_1, D_2) and isotropic (I) moment rate tensor components obtained through inversion by Gilbert and Dziewonski (1975). Details of the geometry of their sources are given in Table III. D_1 is essentially equivalent to the double-couple sources of Mendiguren (1972) and Furumoto and Fukao (1976).

We computed synthetic seismograms for the source models published by Furumoto and Fukao and by Gilbert and Dziewonski, using the mode summation technique discussed above. Fig. 9 shows a comparison of the observed trace (a) (detrended by subtracting the running average) with these synthetics. The synthetic for Furumoto and Fukao's (1976) step-function double-couple (with a moment of $2.1 \cdot 10^{28}$ dyn cm) – shown in trace (b) – is in excellent agreement with the data. In addition to the agreement of the wave shapes and dispersion of

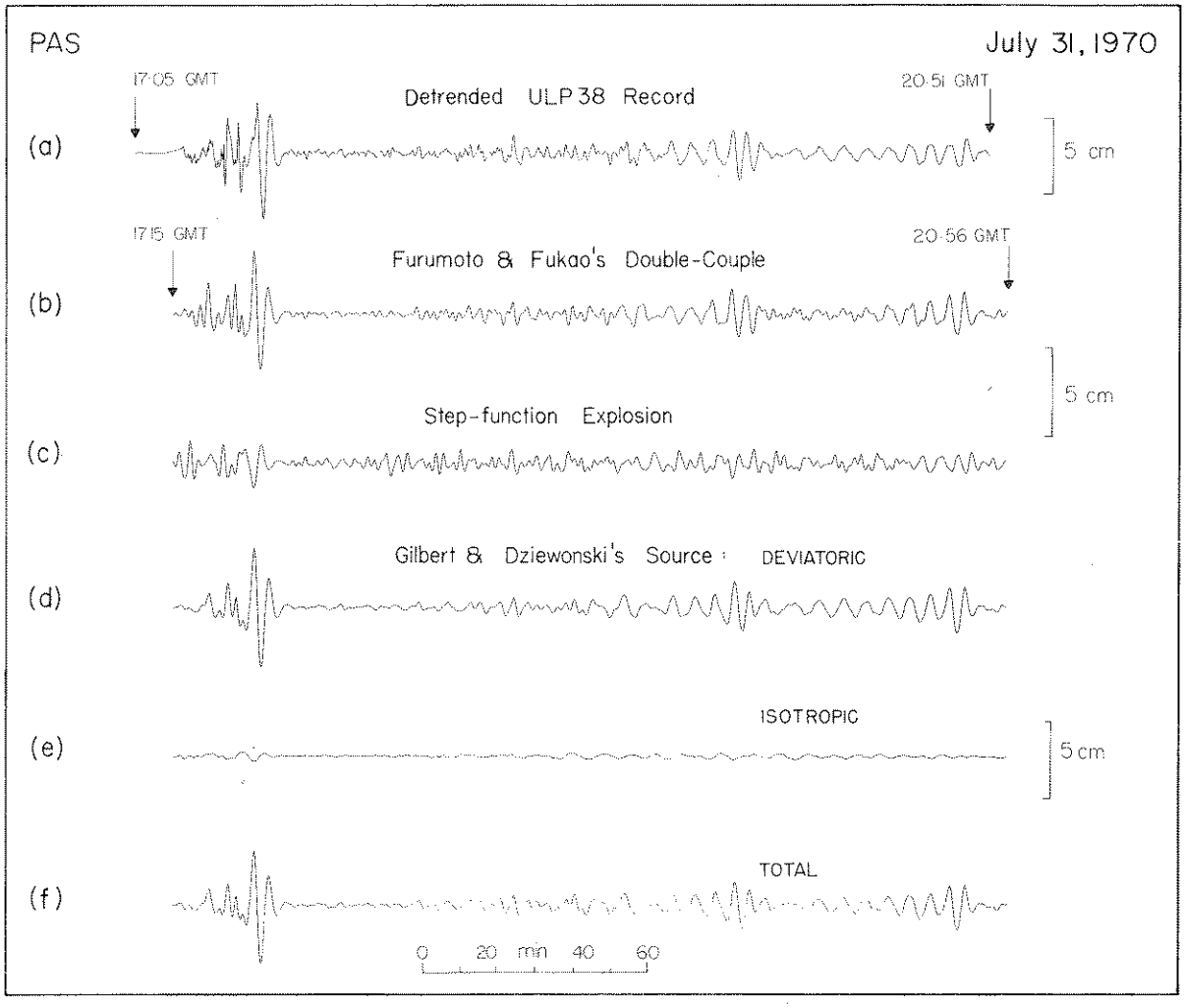

Fig. 9. (a) Detrended trace of the ULP38 record at *PAS*.
(b) Synthetic obtained for Furumoto and Fukao's (1976) source, using a step-function moment $2.1 \cdot 10^{28}$ dyn cm.
(c) Synthetic for an isotropic step-function source of the same moment as (b). (b) and (c) are drawn on the same scale.
(d) Synthetic obtained using only the deviatoric part of the moment rate tensor proposed by Gilbert and Dziewonski (1975).
(e) Synthetic obtained for the isotropic part of the moment rate tensor proposed by Gilbert and Dziewonski.
(f) Synthetic for the total source proposed by Gilbert and Dziewonski [(f) = (d) + (e)]. (d), (e) and (f) are on the same scale.

the fundamental Rayleigh waves R_1, R_2, R_3, and of the second arrival of the first Rayleigh overtone ${}_1R_2$, the general amplitude of the high-frequency content of the later part of the record agrees with the data. For purposes of comparison, trace (c) is the synthetic for a step-function isotropic source, with the same moment as (b). Note that the P to Rayleigh ratio for (c) is much higher than allowed by the actual data.

Traces (d), (e), (f) are synthetics for Gilbert and Dziewonski's (1975) source. Trace (d) is for the entire deviatoric part of their solution (both D_1 and D_2); note that the amplitude of the later, high-frequency, "noise" seems somewhat too low. Trace (e), for Gilbert and Dziewonski's isotropic source I, has much lower amplitude than the deviatoric synthetic. Trace (f), the sum of (d) and (e), is very similar to (d), because (d) has much larger amplitude.

The influence of an isotropic component on the seismogram is studied by constructing linear combinations of synthetics (b) and (c) [and (d) and (e)], with various ratios between isotropic and deviatoric moments. The results are shown in Fig. 10 (Furumoto and Fukao's source) and Fig. 11 (Gilbert and Dziewonski's source). In each of these figures, the upper trace is the original data, low-pass filtered at 80 s, since Gilbert and Dziewonski (1975, p. 216) have indicated that their solution loses significance at higher frequencies; however, this filter hardly changes the ultra-long period record. For each of the 11 other traces, the number at the right gives the fraction of pure compression included in the source (ranging from 1 for a pure implosive source to −1 for a pure explosion, through 0 for the pure deviatoric source):

$$F = M_I/(|M_I| + |M_D|) \tag{8}$$

where M_I is the moment of the isotropic source (positive for an implosion), and M_D that of the deviatoric source. The shape of the signals is very insensitive to even a substantial compressional component. Gilbert and Dziewonski's solution calls for $F = 0.3$, since their isotropic source was multiplied by 3.3 to make the isotropic and deviatoric moments equal. The waveforms in Figs. 10 and 11 are very similar to those for the purely deviatoric case. Note, however, that the phase ${}_2R_2$ (the second arrival of the second Rayleigh wave overtone), identified by the vertical arrow on the top trace, is accurately fit only by the pure deviatoric source (or at most 20% explosion), using Furumoto and Fukao's model.

It is also clear from Figs. 9–11 that Gilbert and Dziewonski's source fails to yield the substantial amplitudes at the shortest (although longer than 80 s) periods, present in the first half of the ultra-long period record. Although this might reflect a loss of significance of their solution with increasing frequency, it might also result from the fact that they were unable to use the first one or two hours of data (generally off-scale on most WWSSN instruments). Since the omission of the first hours of data attenuates the high-frequency part of the spectrum, a correction for Q is required. Gilbert and Dziewonski used the MM8 Q model (Anderson et al., 1965), which was designed to fit the Q's of the fundamental torsional and spheroidal modes, but not overtone

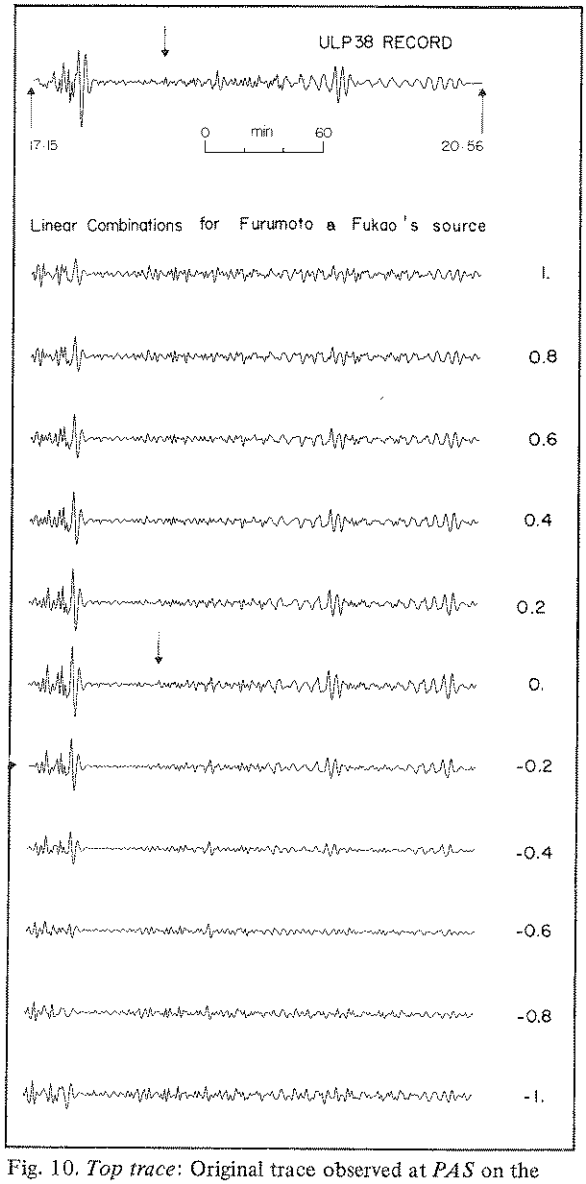

Fig. 10. *Top trace*: Original trace observed at *PAS* on the ULP38 (vertical) instrument, filtered at $T \geqslant 80$ s. *Bottom traces*: Synthetic seismograms for seismic sources ranging from pure implosion (1.0) to pure explosion (−1.0) through pure double-couple (0.0), obtained by taking linear combinations of traces (b) and (c) from Fig. 9. The number on the right is the fraction F described in the text. The scale is the same for all eleven traces, and the total moment is held constant.

data. Any departure of the actual Q from this model could have a strong effect on the higher-frequency content of the spectrum, especially for overtones

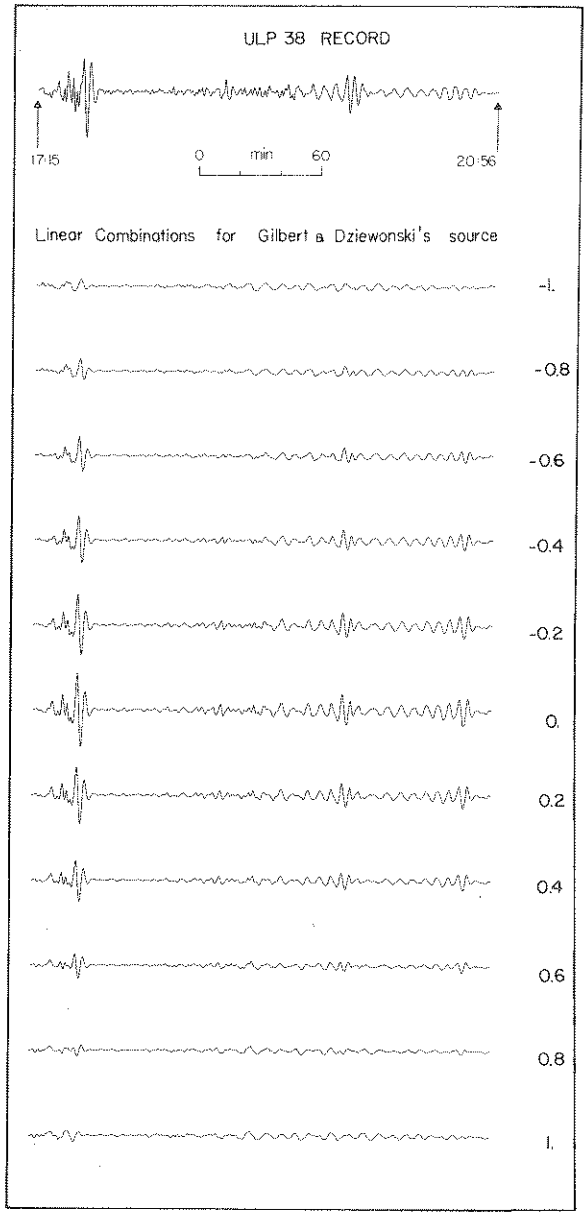

Fig. 11. *Top trace*: Original trace observed at *PAS* filtered at $T \geqslant 80$ s.
Bottom traces: Same as in Fig. 10, except for combinations of (d) and (e) from Fig. 9.

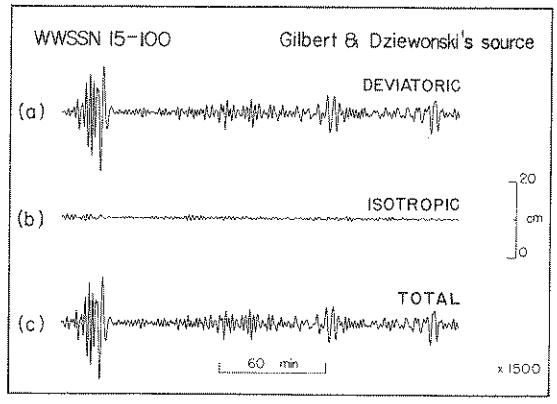

Fig. 12. Synthetic seismograms obtained for Gilbert and Dziewonski's (1975) moment tensor source on a WWSSN instrument. (a): Deviatoric sources D_1 and D_2 only; (b): Isotropic source (I) only; (c): (a) + (b). Records of this type were used by Gilbert and Dziewonski in their moment tensor inversion.

such as the ${}_1R_2$ and ${}_2R_2$ phases.

As we discussed above, the isotropic source does not excite Rayleigh waves efficiently; if the isotropic source were to be resolved by use of a single record, the P waves should be used. A visual comparison of the synthetics suggests that there is very little change in the body-wave traces for $-0.4 \leqslant F \leqslant 0.4$. Therefore, it seems very unlikely that an isotropic source of the size ($F = 0.3$) given by Gilbert and Dziewonski (1975) could actually be resolved from the data at a single station.

These results, strongly suggesting that an isotropic component cannot be resolved from a single high-quality record, are in agreement with the suggestion by Gilbert and Dziewonski (1975), that a stacking and inversion procedure should be used to search for the isotropic source. Fig. 12 shows a synthetic obtained for a standard long-period WWSSN instrument, with the same station geometry as *PAS*, and for Gilbert and Dziewonski's deviatoric sources (a) and implosive source (b). Trace (c) is the total synthetic. The compressional contribution to the WWSSN synthetic is close to negligible, especially after one or two hours, and a single seismogram cannot be used to resolve the isotropic source. This suggests the use of several stations, and inversion procedures. We examine the implications of such an approach below.

4. Least-squares moment tensor inversion

Gilbert and Dziewonski (1975) determined their source mechanism by a least-squares procedure for

finding the moment tensor for the source (Gilbert, 1970), which gives the most general equivalent body forces for a point source (Geller, 1976). As a standard byproduct of the least-squares inversion (Hamilton, 1964), estimates of the variance–covariance matrix for the moment tensor elements are obtained. These statistical estimates of the standard deviation provide one of the compelling arguments advanced by Gilbert and Dziewonski (1975) to support the existence of the isotropic component of the Colombian earthquake. Gilbert and Dziewonski (1975, p. 216) state that:

> "The isotropic part of the [moment] tensor is statistically significant. For a frequency of 0.015 s^{-1} (approximate period of 400 s) we find that 1/3 Re $(M_{rr} + M_{\theta\theta} + M_{\phi\phi}) = -6.0 \times 10^{27}$ dyn cm with a standard error of 6.9×10^{26} dyn cm, thus the inferred value of the isotropic part of the tensor is nearly nine times greater than the standard error. The probability that this would occur by chance alone is less than 10^{-17}."

This is an exceedingly small chance of error: if the quoted standard deviation is indeed established, then the existence of the isotropic source must be accepted.

Gilbert and Dziewonski (1975) used a rather complex scheme for determining the amplitude of each mode; rather than consider that procedure, which they used to obtain their error estimate for the Colombian earthquake quoted above, we will study the more elegant, but essentially equivalent, least-squares technique of Gilbert and Buland (1976). Their paper presents a general scheme for inverting to find the moment tensor as a function of frequency by considering the excitation of the earth's normal modes. Inversion methods for moment tensor determination from body waves have also been developed by Stump (1976) and Strelitz (1977); methods for surface waves have been given by Aki and Patton (1977) and Mendiguren (1977).

The procedure outlined by Gilbert and Buland works as follows: assuming we observe the spectrum $U(\omega_j)$ at several (say P) stations, we then can write the spectrum as:

$$\underline{U}(\omega_j) = H(\omega_j)\,\underline{f}(\omega_j) \tag{9}$$

where $\underline{U}$ is a (complex) P-element column vector, H is a $P \times 6$ (complex) matrix representing the earth's transfer function, which is assumed to be known exactly, and:

$$\underline{f}^T = (M_{rr}, M_{\theta\theta}, M_{\phi\phi}, M_{r\theta}, M_{r\phi}, M_{\theta\phi})$$

is the unknown moment rate tensor. For greater stability we assume that $\underline{f}$ is constant within a frequency band of K distinct frequencies, and get a generalized version of eq. 9:

$$\underline{U} = H\underline{f} \tag{10}$$

which we solve by standard least-squares techniques:

$$\underline{f} = (H^T H)^{-1} H^T \underline{U} \tag{11}$$

In practice, Gilbert and Buland break up $\underline{f}$, $\underline{U}$ and H into their real and imaginary parts and solve for each separately (F. Gilbert, pers. commun., 1977). In that case, $\underline{f}$ has twelve elements, $\underline{U}$ has $2PK$ and H is a $2PK \times 12$ matrix.

From standard least-squares theory, the variance–covariance matrix is given by:

$$\mathrm{VAR} = (H^T H)^{-1}\,\sigma^2 \tag{12}$$

where σ^2 is the variance of an individual observation. Usually σ^2 is unknown, and it is standard practice, which was followed by Gilbert and Dziewonski (1975), to estimate σ^2 from the residuals. One defines:

$$\underline{R} = \underline{U} - H\underline{f} \tag{13}$$

and then:

$$\sigma^2 = \underline{R}^T\underline{R}/(2PK - 12) = (\underline{U}^T\underline{U} - \underline{U}^T H\underline{f})/(2PK - 12) \tag{14}$$

is an unbiased estimate of the variance, which can be used in eq. 12. This is essentially the procedure used by Gilbert and Dziewonski (1975) to obtain their error estimate quoted above.

In the next section, we will carry out a numerical experiment by actually computing the variance–covariance matrix for synthetic seismograms at a group of stations. For that purpose, we define modal amplitude factors, corresponding to the moment tensor components for spheroidal modes:

$$\begin{aligned}
A_{rr} &= \tfrac{1}{6}(K_0 + N_0)P_l^0\,, \\
A_{\theta\theta} &= \tfrac{1}{12}(2N_0 - K_0)\,P_l^0 - \tfrac{1}{4}K_2 P_l^2 \cos 2\phi \\
A_{\phi\phi} &= \tfrac{1}{12}(2N_0 - K_0)\,P_l^0 + \tfrac{1}{4}K_2 P_l^2 \cos 2\phi \\
A_{r\theta} &= -\tfrac{1}{2}K_1 P_l^1 \cos\phi \\
A_{r\phi} &= -\tfrac{1}{2}K_1 P_l^1 \sin\phi \\
A_{\theta\phi} &= -\tfrac{1}{2}K_2 P_l^2 \sin 2\phi
\end{aligned} \tag{15}$$

Due to anelasticity, the contribution of a mode of angular frequency ω_n and quality factor Q_n [whose time dependence is of the form $\exp(-\omega_n t/2Q_n) \cdot \exp(i\omega_n t)$] to a spectrum at angular frequency ω is proportional to its resonance function $C_n(\omega)$:

$$\begin{aligned} \text{Re } C_n(\omega) &= \frac{\omega_n/2Q_n}{(\omega-\omega_n)^2 + \omega_n^2/4Q_n^2} \\ \text{Im } C_n(\omega) &= \frac{(\omega_n - \omega)}{(\omega-\omega_n)^2 + \omega_n^2/4Q_n^2} \end{aligned} \qquad (16)$$

(We do not include the effect of the finite length of records.)

Then, for the vertical component of the spheroidal free oscillations at angular frequency ω, the contribution of a mode to the row of H for the real part of the spectrum, Re $U(\omega)$, is:

$$(A_{rr} \cdot \text{Re } C_n(\omega), -A_{rr} \cdot \text{Im } C_n(\omega), A_{\theta\theta} \cdot \text{Re } C_n(\omega), \ldots) \qquad (17)$$

The imaginary part of the spectrum is:

$$(A_{rr} \cdot \text{Im } C_n(\omega), A_{rr} \cdot \text{Re } C_n(\omega), A_{\theta\theta} \cdot \text{Im } C_n(\omega), \ldots) \qquad (18)$$

[There are, of course PK such "real" rows and PK "imaginary" ones, one for each station, and one for each frequency]. The unknown, $\underline{f}$ has the form:

$$\underline{f}^T = (\text{Re } M_{rr}, \text{Im } M_{rr}, \text{Re } M_{\theta\theta}, \text{Im } M_{\theta\theta}, \ldots) \qquad (19)$$

By summing eqs. 17 and 18 over all modes (over all n), we obtain each full row of H. In practice, we sum only over modes whose C_n is not negligible.

A similar procedure may be applied to the torsional components of U. We define:

$$\begin{aligned} B_{rr} &= 0 \\ B_{\theta\theta} &= \tfrac{1}{4} L_2 \frac{dP_l^2}{d\theta} \sin 2\phi \\ B_{\phi\phi} &= -\tfrac{1}{4} L_2 \frac{dP_l^2}{d\theta} \sin 2\phi = -B_{\theta\theta} \\ B_{r\theta} &= \tfrac{1}{2} L_1 \frac{dP_l^1}{d\theta} \sin\phi \\ B_{r\phi} &= \tfrac{1}{2} L_1 \frac{dP_l^1}{d\theta} \cos\phi \\ B_{\theta\phi} &= -\tfrac{1}{2} L_2 \frac{dP_l^2}{d\theta} \cos 2\phi \end{aligned} \qquad (20)$$

where L_1 and L_2 are the torsional mode excitation coefficients defined by Kanamori and Cipar (1974). We then use the B terms (from eqs. 20) in place of the A terms (from eqs. 15) in eqs. 17 and 18, to obtain the azimuthal components of $\underline{U}$. The fact that $B_{\theta\theta}$ and $B_{\phi\phi}$ do not vanish shows that the information contained in the azimuthal component will reduce the error on the corresponding components ($M_{\theta\theta}$ and $M_{\phi\phi}$) of M, although it will not affect its trace. As a result, the *relative* variance of the isotropic part of the tensor, σ_I^2, will be *increased* with respect to $\sigma^2(M_{\theta\theta})$ and $\sigma^2(M_{\phi\phi})$ by including the torsional data.

5. Standard deviation estimates

Gilbert and Dziewonski's estimate of the standard deviation of the isotropic source is derived from the residuals (eq. 14) between the observed and predicted values of the data, and should be treated with caution. It is well known that such estimates of variance can frequently be unrealistically low, since the model is assumed to be known exactly, and errors in the model (and hence the matrix for the normal equations) are ignored. A classic example of such an unrealistically low estimate of variance is the case of earthquakes in central California, which presumably occurred on the San Andreas Fault, but were consistently located on a plane 1 km to the west of the fault. This error occurred because the flat-layered model used to locate earthquakes did not reflect the actual, laterally heterogeneous, earth structure (Healy and Peake, 1975). Another well-known case is the way that measurements of fundamental physical constants, such as the speed of light or Avogadro's number, have frequently changed by several standard deviations over previous measurements, as systematic biases are eliminated (Particle Data Group, 1971, 1976).

Variance estimates from the residuals assume that the errors in the data are all Gaussian. The model equations, H, are assumed to be known exactly, and possible systematic errors in the model are ignored. Although this procedure is statistically self-consistent, several possible causes of systematic errors in the moment tensor inversion do exist:

(1) Although there are very accurate calibration procedures using random telegraph signals (e.g.,

Moore and Farrell, 1970), the WWSSN calibration is performed by exciting the instrument with a step-function. This causes large uncertainties in the calibration at long periods, where the instrument response is small and decays as T^{-3}. If the calibration is in error at a given station, the signal would most likely be systematically too high or low at all frequencies. Systematic errors at long periods could also be caused by a poor knowledge of the phase response.

(2) The observed spectral data must be corrected for the effects of Q. Lateral heterogeneity or the poorly known overtone Q's could cause systematic errors in the resulting moment tensor.

(3) Most gross earth models are in reasonably good agreement at long periods. However, none of these models fit the observed great-circle group velocities very well, suggesting that further improvement may be needed. Also, the effects of lateral heterogeneity are not included. Uncertainties in the earth model could also cause systematic errors.

6. Numerical experiment

We will conduct numerical tests of the effects of various possible sources of systematic bias on moment tensor inversion. Synthetic spectra are calculated for an earth model including some source of systematic bias such as lateral heterogeneity (using a simple approximation). These synthetic spectra are then inverted to find the moment tensor, *using a laterally homogeneous earth model.*

The synthetic spectra are generated by perturbing the rows of the H matrix given by eqs. 17 and 18 resulting in a new, perturbed, matrix H_p. The perturbed spectra for a particular source are given by $\underline{U} = H_p \underline{f}_0$ where $\underline{f}_0$ is the actual moment tensor for a particular source. Then, the moment tensor obtained from the inversion, $\underline{f}$ is given by:

$$\underline{f} = (H^T H)^{-1} H^T H_p \underline{f}_0 \qquad (21)$$

If H_p were equal to H, then we would find $\underline{f} = \underline{f}_0$. Any discrepancy is due to the perturbation. If the parameters used in the numerical experiment are realistic, then the difference between the moment tensor obtained from the inversion and the original moment tensor should be on the same order as what one would expect in the earth. In particular, we will be interested in the magnitude of the isotropic source produced by a purely deviatoric $\underline{f}_0$.

In all of our experiments to find the effect of different possible perturbations, we will calculate synthetic spectra for a "network" of ten stations, evenly spaced in azimuth from 0° to 360°, at a common epicentral distance of 60° from the source. We calculated the vertical component of spheroidal modes and the azimuthal component of torsional modes (neglecting the azimuthal component of spheroidal modes) at each station. The additional information in the azimuthal component increases the accuracy with which $M_{\theta\theta}$ and $M_{\phi\phi}$ can be determined relative to the accuracy of the moment of the isotropic source (M_I).

6.1. *Lateral heterogeneity*

It is impossible to calculate synthetic spectra exactly for a laterally heterogeneous earth. [In fact, Geller and Stein (1978) have shown that the most obvious approximation technique, first-order perturbation theory, frequently may not give accurate results.] In this study, we will approximate the effect of lateral heterogeneity by assuming that the phase velocity is affected by the heterogeneity, but that the amplitude is not. [We are using a mode expansion in this paper but ω can be related to c by the asymptotic formula $c = \omega a/(l + 1/2)$.]

Most regionalized earth models (e.g., Okal, 1977), show that regional variation in observed great-circle phase velocities can be explained by lateral heterogeneity in only the upper 250 km. Such heterogeneity would affect the fundamental mode of Rayleigh and Love waves most, and would have a smaller effect on overtones. We adopt a very simple model of the effect of "lateral heterogeneity" on eigenfrequencies at a station with azimuth ϕ:

$$ {}_n\omega_l(\phi) = {}_n(\omega_0)_l \left[1 + \cos 2\phi \cdot G \cdot \frac{200\, {}_n(\omega_0)_l}{2\pi} \right] \qquad (22)$$

${}_n(\omega_0)_l$ is the original eigenfrequency and ${}_n\omega_l(\phi)$ is the eigenfrequency of the laterally heterogeneous model at the azimuth ϕ. G is a factor which reduces the strength of the heterogeneity for higher over-

tones:

$$G = \begin{cases} 0.015 & \text{for} \quad n = 0 \\ 0.0075 & \text{for} \quad n = 1 \\ 0.00375 & \text{for} \quad n = 2 \\ 0 & \text{for} \quad n > 2 \end{cases} \qquad (23)$$

From eqs. 22 and 23 the "heterogeneity" increases with increasing frequency and decreases for higher overtones (at 0.005 Hz the heterogeneity is ±1.5% for the fundamental mode, ±0.75% for the first overtone, ±0.375% for the second and 0 for all higher modes, while at 0.01 Hz it is ±3%, ±1.5%, ±0.75% and 0 respectively). Eqs. 22 and 23 are used for both spheroidal and torsional modes. Clearly this model of lateral heterogeneity is schematic. However, it seems sufficient for a test of the effect of lateral heterogeneity on moment tensor inversion.

We obtained a completely artificial isotropic moment from the inversion whenever the coefficient of K_0 (s_R) was non-zero for the original source. As an example, we used the mechanism of the Colombian earthquake found by Mendiguren (1973): $\delta = 58°$ and $\lambda = -99°$ (and arbitrarily set ϕ_s, the fault strike, equal to zero). For this mechanism, the coefficient of K_0 which depends on fault geometry, $s_R = \frac{1}{2} \sin\lambda \sin 2\delta = -0.44$ is close to its maximum absolute value. We found that such a mechanism is most susceptible to the effects of lateral heterogeneity. The results for the inversion are shown in Fig. 13. The moment rate spectrum for Mendiguren's geometry and a step-function source (f_0) are plotted as straight lines. (The step-function time dependence of the source, means that the moment rate spectrum of the theoretical source is flat.) The moment rate spectra obtained from the inversion are plotted as plus signs. It can be seen that even the small heterogeneity implied by eqs. 22 and 23 is enough to cause very large differences between the spectra from the inversion and the original spectra. The original isotropic spectrum was zero, but here the isotropic spectrum resulting from the inversion differs substantially from zero. The standard deviations of the real part of the moment

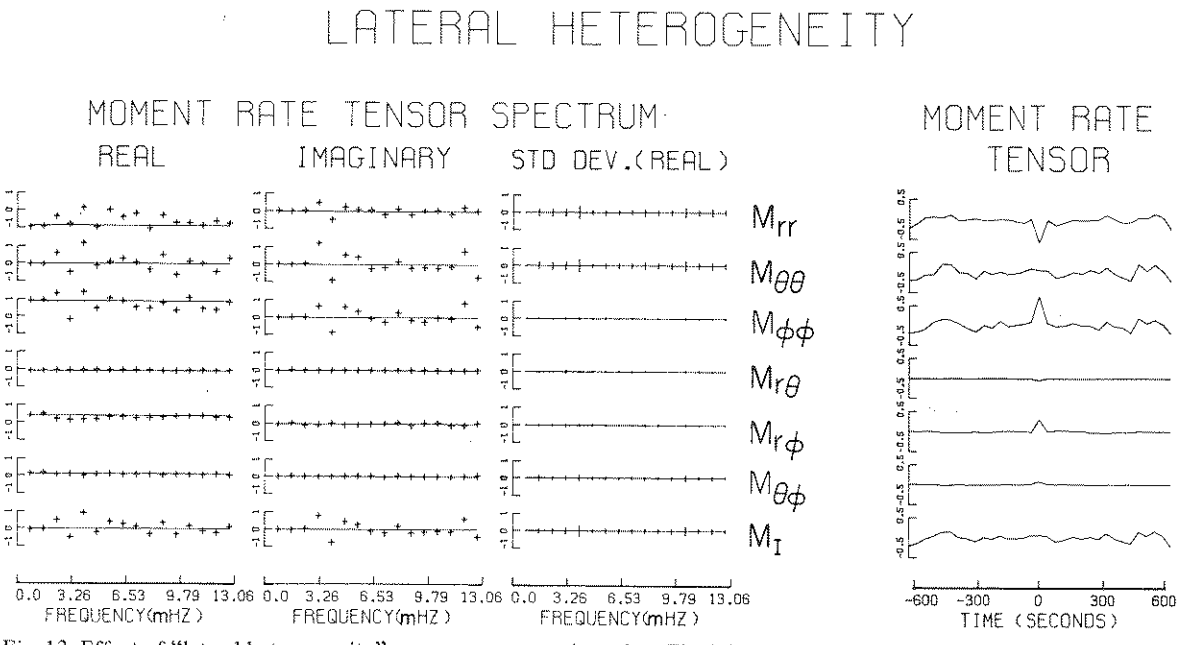

Fig. 13. Effect of "lateral heterogeneity" on moment tensor inversion. The leftmost two columns show the result of the inversion of the data for a "laterally heterogeneous" earth, using a laterally homogeneous model (+ *signs*), and the "correct" moment rates (*straight lines*) which were used to generate the spectra. The third column shows the nominal standard deviations resulting from the inversions. The fourth column shows the moment rate functions in the time domain. Units in the right column are 10^{27} dyn cm s^{-1}. Units in the three leftmost columns are 10^{27} dyn cm. Note the large isotropic source resulting from the inversion.

rate spectrum are shown in the third column (as calculated from eq. 14). At several frequencies, the isotropic spectrum is greater than the standard deviation, and thus statistically significant. (If we had used more than ten stations, the error bars would have been even smaller.) The standard deviation of the isotropic moment rate spectrum shown in Fig. 13 was calculated from the variance–covariance matrix (12), using the formula:

$$\sigma^2_{\text{incomplete}}(M_I) = \tfrac{1}{9}[\sigma^2(M_{rr}) + \sigma^2(M_{\theta\theta}) + \sigma^2(M_{\phi\phi})] \tag{24}$$

which was used by Gilbert and Dziewonski (1975). The formula which should be used is:

$$\sigma^2(M_I) = \tfrac{1}{9}[\sigma^2(M_{rr}) + \sigma^2(M_{\theta\theta}) + \sigma^2(M_{\phi\phi}) + 2\,\mathrm{cov}(M_{rr}, M_{\theta\theta}) + 2\,\mathrm{cov}(M_{rr}, M_{\phi\phi}) + 2\,\mathrm{cov}(M_{\theta\theta}, M_{\phi\phi})] \tag{25}$$

All of the covariance terms are non-zero, and when they are included, the correct value of the standard deviation (from eq. 25) is usually about 50% greater. Table IV lists the values shown in the first three columns of Fig. 13, together with the correct standard deviations from eq. 25.

We investigated the effect of a possible lateral heterogeneity in Q using a formula similar to eq. 22:

$${}_nQ_l(\phi) = {}_n(Q_0)_l\left[1 + \cos 2\phi \cdot G_Q \cdot \frac{200\,{}_n(\omega_0)_l}{2\pi}\right] \tag{26}$$

where

$$G_Q = \begin{cases} 0.30 & \text{for} \quad n = 0 \\ 0.15 & \text{for} \quad n = 1 \\ 0.075 & \text{for} \quad n = 2 \\ 0 & \text{for} \quad n > 2 \end{cases} \tag{27}$$

These values of G_Q are on the order of the lateral variations in Q found by Nakanishi (1977). The results shown in Fig. 14 suggest that lateral variations in Q can be as important as lateral heterogeneity in phase velocity in contributing as a cause of artificial isotropic components from moment tensor inversion. However, although our model of lateral heterogeneity causes spurious isotropic sources to be obtained from the inversion procedure, the phase of our source is not consistent, while the phase of the isotropic component obtained by Gilbert and Dziewonski (1975) was.

TABLE IV

Isotropic component of the moment rate tensor resulting from the inversion in the presence of lateral heterogeneity

Period (s)	Isotropic moment M_I (10^{27} dyn cm)		σ_I (10^{27} dyn cm)	
	real	imaginary	complete	incomplete
1256.6	−0.029	0.017	0.0132	0.0175
628.3	−0.014	−0.002	0.1576	0.1360
418.9	0.510	0.056	0.0987	0.1213
314.2	−0.483	0.778	0.1172	0.1754
251.3	0.905	−0.743	0.1910	0.3091
209.4	−0.210	0.463	0.0819	0.1177
179.5	0.389	0.279	0.0947	0.1544
157.5	0.259	−0.099	0.0847	0.1369
139.6	0.135	−0.209	0.0881	0.1410
125.7	−0.301	0.196	0.1086	0.1420
114.2	0.344	−0.199	0.0909	0.1398
104.7	−0.325	−0.136	0.0939	0.1510
96.7	0.175	−0.076	0.1579	0.2648
89.8	−0.130	−0.129	0.0876	0.1372
83.8	−0.231	0.604	0.1108	0.1589
78.5	0.133	−0.424	0.0768	0.1069

The starting moment used has the geometry of Mendiguren's (1973) source, with a dislocation moment of 10^{27} dyn cm and a step-function time dependence.

We also conducted two other experiments. In the first, the spectra were calculated with instrument magnifications which could vary randomly within ±20% of the nominal value (a conservative estimate for a typical WWSSN station). In the second, Q was assumed to be known accurately for the fundamental modes, but to be 30% systematically lower than SL2 for all the overtones. Neither experiment yielded any significant isotropic source.

7. Discussion

Gilbert and Dziewonski (1975) commented on the very different time functions of the deviatoric and isotropic components of the moment rate tensor. They pointed out that the deviatoric components of the moment tensor were coseismic, and that only

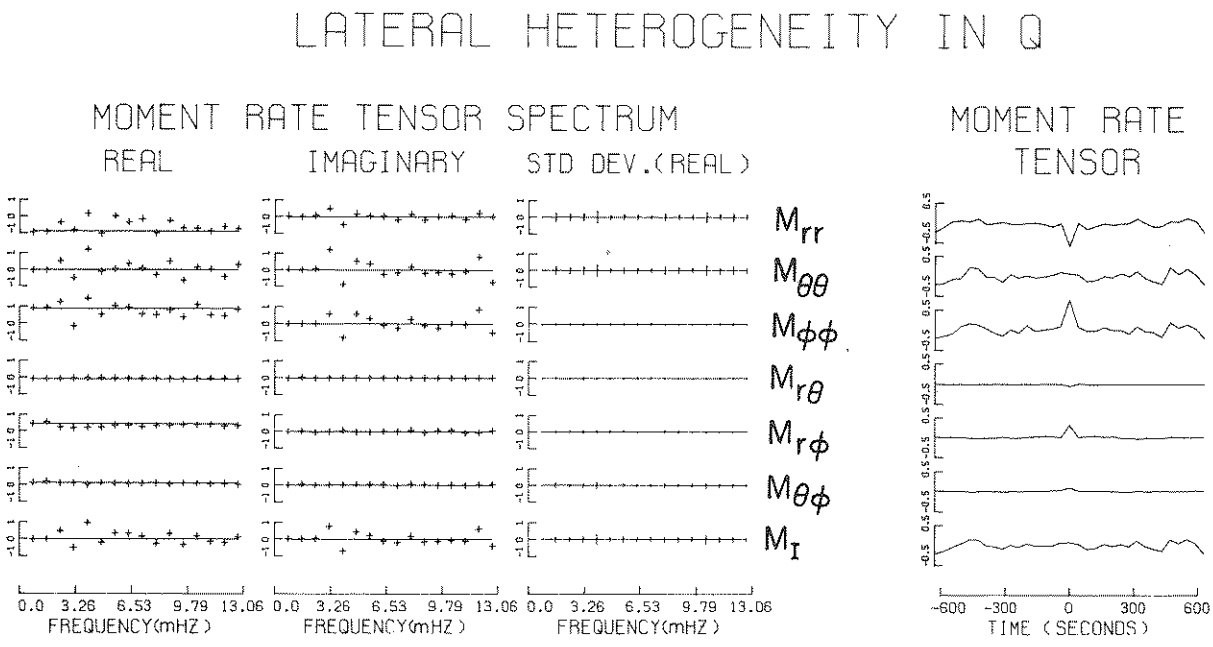

Fig. 14. Same as Fig. 13, for a laterally heterogeneous attenuation factor Q.

the isotropic source was precursory. A somewhat different conclusion can be reached from Fig. 8, in which we present the time functions for particular combinations of the principal components of the moment rate tensor given by Gilbert and Dziewonski (1975, Fig. 27). In Fig. 8, I, the isotropic moment rate function, is the average of the three principal components. D_1 is the moment rate function for a double-couple on a fault plane which is essentially the same as that inferred by Mendiguren (1972). Finally, D_2 is the moment rate function for a double-couple on essentially the plane defined by the T and null axes of Mendiguren's source.

A remarkable difference between the overall time constants of I, D_1 and D_2 emerges from Fig. 8. D_1 has a time constant of about 100 s, but since Gilbert and Dziewonski did not consider data at periods below 80 s, this time function is essentially equivalent to the step-like time function which Mendiguren (1972) and Furumoto and Fukao (1976) also found for the double-couple on this fault plane. On the other hand, both I and D_2 have very long rise times of about 300 s. Moreover, *both* I and D_2 appear to be precursory, in contrast to D_1 which is clearly coseismic, and not precursory.

Since these results were derived from WWSSN instruments which have very poor ultra-long period response (Fig. 6), we might conclude that the source function D_1, which corresponds to the fault plane found by other investigators, is correct and confirmed by the study in Section 3. However, the very large time constant for I and D_2 suggests that the energy for these sources is concentrated at long periods greater than (300 s) at which the response of the WWSSN instrument is extremely poor.

We therefore suggest that I and D_2 are probably the result of noisy data at these long periods, and of systematic errors, as illustrated by the numerical experiment in Section 6.

8. Conclusions

Although the conclusive demonstration of the existence of a deep isotropic source would be an extremely exciting development, we conclude that the precursive isotropic source reported for the Colombian earthquake is unresolvable. Although we present results which differ from those obtained by Gilbert and Dziewonski (1975), they presented

for the first time a systematic method for using all the available data to determine the source mechanism. As better long-period data, with a higher signal/noise ratio, become available (Agnew et al., 1976; Peterson and Orsini, 1976), it should become possible to reach a definite conclusion regarding the existence or non-existence of isotropic seismic sources.

Acknowledgments

We thank Katsuyuki Abe, Keiiti Aki, Don L. Anderson, Adam Dziewonski, Freeman Gilbert, Hiroo Kanamori and Seth Stein for helpful discussions and comments. Ray Buland, Freeman Gilbert and Bob Hart calculated the excitation coefficients for the normal modes. Muneyoshi Furumoto and Ichiro Nakanishi kindly sent preprints prior to publication. This work was supported by National Science Foundation Grants Nos. EAR77-14675 and EAR78-11973 at Caltech and by National Science Foundation Grant EAR78-03653 at Stanford. Contribution Number 2991, Division of Geological and Planetary Sciences, California Institute of Technology.

References

Abe, K., 1970. Determination of seismic moment and energy from the earth's free oscillations, Phys. Earth Planet. Inter., 4: 49–61.

Agnew, D., Berger, J., Buland, R., Farrell, W. and Gilbert, F., 1976. International deployment of accelerometers: a network for very long period seismology. EOS (Trans. Am. Geophys. Union), 57: 180–188.

Aki, K. and Patton, H., 1977. Determination of seismic moment tensor using surface waves. EOS (Trans. Am. Geophys. Union), 58: 441 (abstract).

Alterman, Z., Jarosch, H. and Pekeris, C.L., 1959. Ocillations of the earth. Proc. R. Soc. London, Ser. A, 252: 80–95.

Anderson, D.L. and Hart, R.S., 1976. An earth model based on free oscillations and body waves. J. Geophys. Res., 81: 1461–1475.

Anderson, D.L. and Hart, R.S., 1978. Attenuation models of the earth. Phys. Earth Planet. Inter., 16: 289–306.

Anderson, D.L., Ben-Menahem, A. and Archambeau, C.B., 1965. Attenuation of seismic energy in the upper mantle. J. Geophys. Res., 70: 1441–1448.

Benioff, H., 1964. Earthquake source mechanisms. Science, 143: 1399–1406.

Chung, W.Y. and Kanamori, H., 1976. Source process and tectonic implications of the Spanish deep-focus earthquake of March 29, 1954. Phys. Earth Planet. Inter., 13: 85–96.

Dennis, J.G. and Walker, C.T., 1965. Earthquake resulting from metastable phase transitions. Tectonophysics, 2: 401–407.

Dratler, J., Farrell, W.E., Block, B. and Gilbert, F., 1971. High-Q overtone modes of the Earth. Geophys. J.R. Astron. Soc., 23: 399–410.

Dziewonski, A.M. and Gilbert, F., 1974. Temporal variation of the seismic moment tensor and the evidence of precursive compression for two deep earthquakes. Nature (London), 247: 185–188.

Fukao, Y., 1971. Seismic body waves from surface faults. J. Phys. Earth, 19: 271–281.

Fukao, Y. and Abe, K., 1971. Multimode love waves excited by shallow and deep earthquakes. Bull. Earthquake Res. Inst., Tokyo Univ., 49: 1–12.

Furumoto, M., 1977. Spacio-temporal history of the deep Colombia earthquake of 1970. Phys. Earth Planet. Inter., 15: 1–12.

Furumoto, M. and Fukao, Y., 1976. Seismic moment of great deep shocks. Phys. Earth Planet. Inter., 11: 352–357.

Geller, R.J., 1974. Evidence of precursive compression for two deep earthquakes. Nature (London), 252: 28–29.

Geller, R.J., 1976. Body force equivalents for seismic stress drop sources. Bull. Seismol. Soc. Am., 66: 1801–1804.

Geller, R.J. and Stein, S., 1978. Normal modes of a laterally heterogeneous body: a one-dimensional example. Bull. Seismol. Soc. Am., 68: 103–116.

Gilbert, F., 1970. Excitation of the normal modes of the earth by earthquakes and explosions. Geophys. J., 22: 223–226.

Gilbert, F. and Buland, R., 1976. An enhanced deconvolution procedure for retrieving the seismic moment tensor from a sparse network, Geophys. J., 47: 251–255.

Gilbert, F. and Dziewonski, A.M., 1975. An application of normal mode theory to the retrieval of structural parameters and source mechanisms from seismic spectra. Philos. Trans. R. Soc. London, Ser. A, 278: 187–269.

Gilman, R., 1960. Report on some experimental long-period systems. Bull. Seismol. Soc. Am., 50: 553–559.

Hamilton, W.C., 1964. Statistics in Physical Science. Ronald Press, New York, N.Y.

Harkrider, D.G., 1964. Surface waves in multilayered elastic media, I. Rayleigh and Love waves from buried sources in a multilayered elastic half-space. Bull. Seismol. Soc. Am., 54: 627–679.

Hart, R.S. and Kanamori, H., 1975. Search for compression before a deep earthquake. Nature (London), 253: 333–336.

Healy, J.H. and Peake, L.G., 1975. Seismic velocity structure along a section of the San Andreas Fault near Bear Valley, California. Bull. Seismol. Soc. Am., 65: 1177–1197.

Jeffreys, H., 1928. The times of transmission and focal depths of large earthquakes. Mon. Not. R. Astron. Soc., Geophys. Suppl., 1: 500–521.

Kanamori, H. and Cipar, J., 1974. Focal process of the great Chilean earthquake of May 22, 1960. Phys. Earth Planet. Inter., 9: 128–136.

Kanamori, H. and Stewart, G.S., 1976. Mode of strain release along the Gibb's fracture zone, Mid-Atlantic Ridge. Phys. Earth Planet. Inter., 11: 312–332.

Kennett, B.L.N. and Simons, R.S., 1976. An implosive precursor to the Colombia earthquake 1970 July 31. Geophys. J.R. Astron. Soc., 44: 471–482.

Landisman, M., Usami, T., Satô Y. and Massé, R., 1970. Contributions of theoretical seismograms to the study of modes, rays and the earth. Rev. Geophys. Space Phys., 8: 533–589.

Langston, C.A. and Helmberger, D.V., 1975. A procedure for modeling shallow dislocation sources, Geophys. J., 42: 117–130.

Matuzawa, T., 1964. Study of Earthquakes. Uno Shoten, Tokyo.

Mendiguren, J.A., 1972. Source mechanism of a deep earthquake from analysis of world-wide observations of free oscillations. Ph.D. Thesis, Massachusetts Institute of Technology, Cambridge, Mass.

Mendiguren, J.A., 1973. Identification of free oscillation spectral peaks for 1970 July 31, Colombian deep shock using the excitation criterion. Geophys. J., 33: 281–321.

Mendiguren, J.A., 1975. Volumetric characteristics of the focal process of deep earthquakes based on free oscillation data. EOS, (Trans. Am. Geophys. Union), 56: 1028 (abstract).

Mendiguren, J.A., 1977. Inversion of surface wave data in source mechanism studies. J. Geophys. Res., 82: 880–894.

Moore, R.D. and Farrell, W.E., 1970. Linearization and calibration of electrostatically feedback gravity meters. J. Geophys. Res., 75: 928–932.

Nakanishi, I., 1977. Measurements of phase velocities and *Q*. M.S. Thesis, Nagoya University, Nagoya.

Okal, E.A., 1977. The effect of intrinsic oceanic upper-mantle heterogeneity on regionalization of very long period Rayleigh wave phase velocities. Geophys. J.R. Astron. Soc., 49: 357–370.

Okal, E.A., 1978. A physical classification of the Earth's spheroidal modes. J. Phys. Earth, 26: 75–103.

Particle Data Group, 1971. Review of particle properties. Rev. Mod. Phys., 43: S1–S150.

Particle Data Group, 1976. Review of particle properties. Rev. Mod. Phys., 48: S1–S305.

Peterson, J. and Orsini, N.A., 1976. Seismic research observatories: Upgrading the worldwide seismic data network. EOS (Trans. Am. Geophys. Union), 57: 548–556.

Phinney, R.A. and Burridge, R., 1973. Representation of the elastic-gravitation excitation of a pherical Earth model by generalized spherical harmonics. Geophys. J.R. Astron. Soc., 34: 451–487.

Randall, M.J. and Knopoff, L., 1970. The mechanisms of the focus of deep earthquakes. J. Geophys. Res., 75: 4965–4976.

Saito, M., 1967. Excitation of free oscillations and surfaces by a point source in vertically heterogeneous Earth. J. Geophys. Res., 72: 3689–3699.

Stoneley, R., 1931. On deep-focus earthquakes. Gerlands Beitr. Geophys., 29: 417–435.

Strelitz, R.A., 1977. Source progress of three complex deep earthquakes. Ph.D. Thesis, Princeton University, Princeton, N.J.

Strelitz, R.A., 1978. Moment tensor inversions and source models. Geophys. J.R. Astron. Soc., 52: 359–364.

Stump, B.W., 1976. The determination of source mechanisms by the linear inversion of seismograms. EOS (Trans. Am. Geophys. Union), 57: 953 (abstract).

Sykes, L.R., 1968. Deep earthquakes and rapidly running phase changes – a reply to J.G. Dennis and C.T. Walker. J. Geophys. Res., 73: 1508–1510.

Takeuchi, H. and Saito, M., 1972. Seismic surface waves. Methods Comput. Phys., 11: 217–295.

Vaišnys, J.R. and Pilbeam, C.C., 1976. Deep earthquake initiation by phase transformations. J. Geophys. Res., 81: 985–988.